

Title Page

**Enalapril treatment alters the contribution of EETs but not gap junctions to
EDHF activity in mesenteric arteries of spontaneously hypertensive rats**

Anthie Ellis, Kenichi Goto, Daniel J. Chaston, Therese D. Brackenbury, Kate R.
Meaney, J. R. Falck, Richard J. H. Wojcikiewicz and Caryl E. Hill

Division of Neuroscience, John Curtin School of Medical Research, Australian National
University, Canberra, ACT, 0200, Australia (AE, KG, DC, TDB, KRM, CEH),
Department of Biochemistry, Southwestern Medical Centre, University of Texas,
Dallas, TX (JRF), Department of Pharmacology, State University of New York Upstate
Medical University, Syracuse, New York, 13210-2339 (RJHW).

Running Title Page

Running Title: Myoendothelial gap junctions, EETs and EDHF

Author for correspondence: Professor Caryl E. Hill,
Division of Neuroscience,
John Curtin School of Medical Research,
Australian National University,
Canberra ACT 0200
Australia,
Phone: 61 2 6125 2996;
FAX: 61 2 6125 8077
Email: caryl.hill@anu.edu.au

Number of pages: 38

Tables: 6

Figures: 8

References: 40

Abstract: 248

Introduction: 575

Discussion: 1539

Abbreviations: EDHF, endothelium-derived hyperpolarizing factor; WKY, Wistar-Kyoto; SHR, spontaneously hypertensive rat; 14,15-EEZE, 14,15-epoxyeicosa-5(Z)-enoic acid; EET, epoxyeicosatrienoic acid; K_{Ca} , calcium dependent potassium channels; MEGJ, myoendothelial gap junction; L-NAME, N^G -nitro-L-arginine methyl ester; ODQ, 1H-[1,2,4]oxadiazolo[4,3-a]quinoxalin-1-one; ACh, acetylcholine; IbTx, iberiotoxin; K_{ATP} , ATP dependent potassium channel; 1-EBIO, 1-ethyl-2-benzimidazolinone; TRAM-34, 1-[(2-chlorophenyl)diphenylmethyl]-1H-pyrazole; IP_3 , inositol trisphosphate; Cx, connexin; IEL, internal elastic lamina.

Section assignment: Cardiovascular

Abstract

Reduction in endothelium-derived hyperpolarizing factor (EDHF)-mediated dilatory function in large, elastic arteries during hypertension is reversed following blood pressure normalisation. We investigated whether similar mechanisms occurred in smaller mesenteric resistance arteries from aged WKY, spontaneously hypertensive rats (SHR) and SHR treated with the angiotensin-converting enzyme inhibitor, enalapril, using immunohistochemistry, serial-section electron microscopy, electrophysiology and wire myography. Unlike the superior mesenteric artery, EDHF relaxations in muscular mesenteric arteries were not reduced in SHR, although morphological differences were found in the endothelium and smooth muscle. In WKY, SHR and enalapril-treated SHR, relaxations were mediated by small, large and intermediate conductance calcium-activated potassium channels, which were distributed in the endothelium, smooth muscle, and both layers, respectively. However, only WKY hyperpolarisations and relaxations were sensitive to gap junction blockers and these arteries expressed more endothelial and myoendothelial gap junctions than arteries from SHR. Responses in WKY, but not SHR, were also reduced by inhibitors of epoxyeicosatrienoic acids (EETs), 14,15-EEZE and miconazole, although sensitivity to EET regioisomers was endothelium independent in all rats. Enalapril treatment of SHR reduced blood pressure and restored sensitivity to 14,15-EEZE, but not to gap junction blockers, and failed to reverse the morphological changes. In conclusion, the mechanisms underlying EDHF in muscular mesenteric arteries differ between WKY and SHR, with gap junctions and EETs involved only in WKY. However, reduction of blood pressure in SHR with enalapril restored a role for EETs, but not gap junctions, without reversing morphological changes, suggesting a differential control of chemical and structural alterations.

Introduction

The endothelium of arteries plays a critical role in the regulation of vascular tone by activating vasodilator pathways, the principal mediators being nitric oxide, prostaglandins and endothelium derived hyperpolarising factor (EDHF). The action of EDHF depends on hyperpolarisation and relaxation of smooth muscle cells that is initiated in the endothelium with a rise in intracellular calcium, activation of small (SK_{Ca}) and intermediate conductance (IK_{Ca}) calcium dependent potassium channels and hyperpolarisation of the endothelial membrane. Although the mechanism by which endothelial hyperpolarisation is transduced to smooth muscle hyperpolarisation is still controversial and may vary amongst different vascular beds and species, there is developing consensus that both contact-mediated and diffusible pathways exist (see reviews (Triggle et al., 2003; Griffith et al., 2004; Sandow et al., 2004; Feletou and Vanhoutte, 2006).

For a contact-mediated mechanism to underlie EDHF, gap junctions must link the endothelium with the inner layer of smooth muscle. Indeed, a close correlation exists between the incidence of myoendothelial gap junctions (MEGJs) and EDHF in a number of arteries of different size and morphology (Sandow and Hill, 2000; Sandow et al., 2002; Sandow et al., 2003; Sandow et al., 2004) and EDHF is blocked in small mesenteric arteries following pinocytotic loading of endothelial cells with antibodies against connexin40, a component of MEGJs in this vessel (Mather et al., 2005). Further proof of the involvement of MEGJs in the action of EDHF has emerged through the use of gap junction uncouplers (Griffith et al., 2004). Although many such antagonists have been discredited (Chaytor et al., 1997; Tare et al., 2002), the gap peptides which mimic extracellular connexin sequences are reported to act in a gap junction specific manner (Matchkov et al., 2006). With regard to diffusible elements, endothelial release of the

arachidonate metabolites, epoxyeicosatrienoic acids (EETs), represents a viable mechanism by which a transferable factor could elicit a smooth muscle hyperpolarisation and relaxation, through the opening of BK_{Ca} channels, perhaps via activation of TRP channels (Loot et al., 2008; Zhang et al., 2009).

In hypertension, endothelial dysfunction occurs through deficits in both nitric oxide and EDHF (Goto et al., 2004b; Yang and Kaye, 2006). In the large, elastic, superior mesenteric artery of aged spontaneously hypertensive rats (SHR), which represent a model of angiotensin II-dependent hypertension, EDHF-mediated hyperpolarisation and relaxation is severely attenuated, but completely restored and even augmented following inhibition of the renin-angiotensin system (Goto et al., 2000; Goto et al., 2004a). Our aim was therefore to determine whether similar changes in EDHF were found in the smaller resistance vessels of the mesenteric circulation and whether they were accompanied by alterations to myoendothelial coupling and the involvement of gap junctional mechanisms. Since our previous studies demonstrated no change in the incidence of MEGJs in the caudal artery of SHR, where there was no deficit of EDHF (Sandow et al., 2003), we hypothesised that any reduction in EDHF-mediated dilation would be accompanied by diminished myoendothelial coupling and that antihypertensive treatment would improve dilation and be accompanied by a greater prominence of MEGJs and gap junction-dependent mechanisms. However, in contrast to the superior mesenteric artery, our data did not demonstrate any differences in the sensitivity of EDHF-mediated dilatory responses amongst muscular mesenteric arteries taken from aged WKY, SHR or enalapril-treated SHR, but we did uncover differences in the expression of endothelial and myoendothelial gap junctions and alterations in the involvement of gap junctions and eicosanoids in the mechanisms recruited by the different rat groups to elicit EDHF dilation.

Methods

Experiments involved 11-12 month-old male WKY rats and age-matched SHR and were conducted under a protocol approved by the Animal Experimentation and Ethics Committees of the Australian National University, Canberra. Some groups of 9-10 month old SHR rats were treated for 8 weeks with enalapril (35mg/kg/day in the drinking water) as used previously (Goto et al., 2000). Blood pressure measurements were taken in conscious animals using tail cuff plethysmography, with the average of four readings taken as the representative systolic blood pressure for a given rat.

Electrophysiology and Myography

Rats were anaesthetized with ether, decapitated and the primary mesenteric or first order arteries, originating from the superior mesenteric artery and supplying the ileum, were removed and cut into short segments for either intracellular electrophysiological recordings or isometric tension studies. All experiments were conducted in the presence of L-NAME (100 μ M) and indomethacin (10 μ M) to eliminate the contribution of nitric oxide and prostanoids, respectively. In some experiments, ODQ (10 μ M) was present with other drugs to ensure complete blockade of nitric oxide, although preliminary experiments showed that ODQ did not produce any additional inhibitory effects to those of L-NAME.

For electrophysiological studies, segments (10mm) were pinned in a recording chamber and superfused with Krebs solution containing (mM): 120 NaCl; 5 KCl; 25 NaHCO₃; 1 NaH₂PO₄; 2.5 CaCl₂; 2 MgCl₂; 11 glucose; gassed with 95 % O₂ and 5% CO₂, maintained at 33 – 34°C. Intracellular recordings of membrane potential were made with an Axoclamp 2B (Axon Instruments), using sharp microelectrodes (120-180M Ω) filled with propidium iodide (0.2% in 0.5 M KCl) advanced from the adventitial surface of the arterial segments. All intracellular recordings were made from

smooth muscle cells identified by dye labeling. Hyperpolarisation to ACh (1 μ M) was measured in the presence or absence of phenylephrine (1 μ M), using preparations taken from different rats. Additional preparations were used to measure responses to ACh before and after incubation in the EET analogue 14,15-EEZE (10 μ M) for 15 min, or a combination of the connexin mimetic peptides, ^{37,43}gap 27, ⁴⁰gap 27 and ⁴³gap 26 (100 μ M each), for 1 h. Hyperpolarisations to the ATP dependent potassium channel (K_{ATP}) opener, levcromakalim (0.3, 10 μ M), and the IK_{Ca} opener, 1-EBIO (30, 600 μ M) were also recorded.

For isometric tension studies, segments (1 mm) were mounted on tungsten wires (40 μ m) in a wire myograph (Model 510A, Danish Myo Technology) and stretched to the equivalent of 80 mm Hg during normalisation. Vessels were equilibrated for 30 min and then precontracted with concentrations of phenylephrine (0.3 – 1 μ M) which produced submaximal constrictions of 70-80% of the maximum constriction obtained in each vessel. Responses to the cumulative addition of ACh (0.001 – 3 μ M) were investigated in the absence and presence of the connexin mimetic peptide combination, ^{37,43}gap 27, ⁴⁰gap 27 and ⁴³gap 26 (100 μ M each), K_{Ca} channel inhibitors; iberiotoxin (IbTx 100 nM), apamin (500 nM) and TRAM-34 (500 nM; kindly supplied by Dr H. Wulff); catalase (2000 U/ml), the EET analogue 14,15-EEZE (10 μ M) and the cytochrome P450 epoxygenase inhibitor, miconazole (1 μ M). Gap peptides were preincubated for 1 h, TRAM-34 for 30 mins, whereas all other drugs were preincubated for 10-15 min.

The dose dependent dilatory effects of the regioisomer epoxyeicosatrienoic acids, 5,6-EET; 8,9-EET; 11,12-EET; 14,15-EET (0.01 – 10 μ M; synthesized by the laboratory of J.R. Falck) and of the potassium channel openers, levcromakalim and 1-EBIO, were also recorded amongst the rat groups. The effect of EEZE (10 μ M),

miconazole (1 μ M) and the K_{ATP} inhibitor, glibenclamide, (10 μ M) on dilations to ACh and levcromakalim were determined to rule out the involvement of K_{ATP} channels in the actions of EEZE and miconazole.

In some preparations, the endothelium was removed by gently rubbing a small feather through the lumen. Successful removal of endothelium was confirmed by the failure of 1 μ M ACh to induce a dilation.

Immunohistochemistry

Rats were anaesthetized as above, perfused with saline containing 0.1% bovine serum albumin, 0.1% $NaNO_3$, 5 U/ml heparin (60 mmHg), and either fixed with 2% paraformaldehyde (0.1 M sodium phosphate buffer,) and arteries processed as whole mounts (Grayson et al., 2004; Rummery et al., 2005), or arteries were embedded in OCT (Tissue Tek, USA) and 10 μ m sections cut on a cryostat. The following antibodies were diluted in phosphate buffered saline containing 2% bovine serum albumin, 0.2% Triton-X100: rabbit anti- SK_{Ca} (1:200, APC-025, Alomone Labs), rabbit anti- IK_{Ca} (1:100, APC-064, Alomone Labs), rabbit anti- IK_{Ca} (1:100, kindly supplied by C.B. Neylon; see (Neylon et al., 2004) for antibody characterisation), rabbit anti- BK_{Ca} (1:50, APC-021, Alomone Labs), rabbit anti- IP_3 receptor subtypes I (1:50), II (1:10) (Wojcikiewicz, 1995), mouse anti- IP_3 receptor subtype III (1:50, BD Transduction Labs), sheep anti-connexin37 (Cx37, 1:100, (Grayson et al., 2004; Rummery et al., 2005)), sheep anti-Cx40 (1:100, (Grayson et al., 2004; Rummery et al., 2005)) and rabbit anti-Cx43 (1:100, Zymed). Staining was visualized using Cy3 conjugated goat anti-rabbit, donkey anti-mouse or donkey anti-goat antibodies (1:100, 1:100, 1:300, respectively; Jackson Immunoresearch Laboratories) and image series collected at 0.3 μ m with a BioRad Radiance 2000 confocal microscope. Specificity of antibodies was tested by omission of the primary antibody or preincubation of the primary antibody

with a ten-fold excess of the immunogenic peptide for 1 h at room temperature, prior to application to the tissue.

Quantification of the number of holes in the internal elastic lamina (IEL) was made possible in whole mount preparations due to autofluorescence with 488nm excitation. Since staining for IK_{Ca} channels has been shown to be localized within holes in the IEL at the site of MEGJs (Sandow et al., 2006), antibodies against IK_{Ca} channels were used to localize myoendothelial projections. Whole mount preparations were also stained with antibodies against the IP_3 receptor subtypes I-III, as the IP_3 pathway is integral to the actions of ACh (Goto et al., 2007) and recent studies have implicated these stores in myoendothelial signaling (Isakson et al., 2007). To determine the incidence of expression of IK_{Ca} channels or IP_3 receptors on myoendothelial projections within the IEL of whole mount preparations, optical confocal series were taken of both immunohistochemical staining and the IEL from the level of the endothelium through to the inner surface of the smooth muscle. Sections containing the IEL were projected to a single image and recombined with single confocal images taken above the level of the IEL, close to the smooth muscle (see dotted line marked A, B in Figure 7A). Counts of the number of holes in the IEL containing punctate staining were made from these images. The position of the puncta in the single confocal image, as being above the level of the endothelial cell layer, was verified by following each dot through the confocal z-stack to confirm its position relative to the cellular endothelial staining.

Quantification of Cx staining in the endothelium was undertaken using confocal image series taken through the endothelium of whole mount preparations which were subsequently projected to a single image and analysed using ImageJ (NCBI). Three separate image fields were analysed from each preparation. Preparations were made from 3 to 4 rats representing each of the three rat groups. Endothelial cell sizes were

measured after staining with anti-Cx40, which highlights cellular perimeters (Grayson et al., 2004; Rummery et al., 2005).

Electron Microscopy

Rats were anaesthetized with 44 and 8 mg/kg ketamine and xylazine (i.p.) respectively and processed as previously described (Sandow and Hill, 2000). Serial sections covering 5 μm of each vessel were examined along the IEL to locate MEGJs which were identified by the presence of pentalaminar membrane. Potential MEGJs, where pentalaminar membrane was not discernable but there was no detectable gap between smooth muscle and endothelial membranes, were also counted. The number of smooth muscle cell layers was determined by averaging four measurements 90° apart for each vessel.

Statistical Analysis

Statistical significance was tested using one-way or two-way ANOVA, followed by unpaired *t* tests with Bonferroni modification for multiple groups as appropriate. Data are presented as means and SEM. Numbers represent preparations, each taken from a different rat;. A *P* value < 0.05 was taken to denote significance.

Results

Blood pressure of SHR was significantly higher than that of WKY rats (SHR 196 \pm 3 mmHg, n=16; WKY 137 \pm 4 mmHg, n=11; *P*<0.05). Treatment of SHR with enalapril successfully reduced blood pressure (117 \pm 3 mmHg, n=21; *P*<0.05, one-way ANOVA). Blood pressure of enalapril-treated SHR was significantly lower than that of WKY.

Role of K_{Ca} channels in EDHF Responses

Maximal constrictions to phenylephrine (0.1 – 10 μ M) were significantly greater in SHR than in enalapril-treated counterparts and WKY, although the sensitivity did not differ between the different rat groups (Maximal constrictions and pD_2 values respectively - WKY: 8.3 ± 2.1 mN, -6.3 ± 0.2 ; SHR: 19.7 ± 1.8 mN, -6.1 ± 0.1 ; SHR+enalapril: 11.3 ± 1.4 mN, -6.1 ± 0.1 ; n=4 - 12). ACh (0.001 – 3 μ M) reversed the constriction produced by submaximal concentrations of phenylephrine (0.3 – 1 μ M) in all three rat groups without significant difference in pD_2 values or peak amplitude of relaxation (maximum), respectively, amongst the groups (WKY: -7.9 ± 0.1 , $97.8 \pm 0.5\%$, n=34; SHR: -7.8 ± 0.1 , $97.3 \pm 0.7\%$, n=24; SHR+enalapril: -7.8 ± 0.1 , $97.7 \pm 1.0\%$, n=18). In order to determine whether differences existed in the time course of dilation amongst the groups, the sustained response which persisted after the initial peak response was also analysed. No significant difference was found in pD_2 values or peak amplitude of relaxation of the sustained response amongst the groups (WKY: -7.7 ± 0.1 , $97.9 \pm 1.8\%$, n=25; SHR: -7.8 ± 0.1 , $98.4 \pm 2.1\%$, n=21; SHR+enalapril: -7.7 ± 0.1 , $98.7 \pm 2.6\%$, n=18).

In the absence or presence of phenylephrine (1 μ M), the resting membrane potential of smooth muscle cells was not significantly different amongst the three rat groups, phenylephrine producing about 10 mV depolarization (Table 1). ACh (1 μ M) induced a hyperpolarisation in all three groups. The amplitude of hyperpolarisation in SHR was significantly smaller than in WKY but was restored in enalapril-treated SHR to values comparable to those in WKY (Table 1).

Both levcromakalim (K_{ATP} opener) and 1-EBIO (IK_{Ca} channel opener) caused concentration dependent hyperpolarisations and relaxations that did not differ between WKY and SHR (pD_2 values for relaxations to levcromakalim: WKY: -6.8 ± 0.2 , n=4;

SHR: -6.8 ± 0.2 , $n=4$; hyperpolarisations to 10^{-5} M: WKY: -27 ± 1.5 mV, $n=4$; SHR: -27 ± 1.4 mV, $n=4$; pD_2 values for relaxations to 1-EBIO: WKY: -4.2 ± 0.1 , $n=4$; SHR: -4.4 ± 0.2 , $n=4$; hyperpolarisations to 3×10^{-4} M: WKY: -19 ± 0.9 mV, $n=3$; SHR: -18 ± 3.5 mV, $n=3$), indicating no impairment in the ability of either smooth muscle or endothelial K channels, respectively, to elicit hyperpolarisation and relaxation.

Blockers of calcium-activated potassium channels, namely the small (SK_{Ca} , apamin 500 nM) and intermediate conductance channels (IK_{Ca} , TRAM-34 500 nM) in the presence of 10 μ M ODQ, significantly shifted ACh curves to the right in all three rat groups. Addition of the large conductance K_{Ca} blocker iberiotoxin (IbTx 100 nM) abolished relaxations, although a small residual relaxation persisted in the WKY group (Figure 1).

Immunohistochemical staining for SK_{Ca} , IK_{Ca} and BK_{Ca} channels demonstrated that the channels were differentially distributed between the endothelium and smooth muscle, however there was no difference in expression amongst the rat groups. Thus, SK_{Ca} expression was confined to the endothelium (Figure 2A-C), BK_{Ca} expression was confined to the smooth muscle (Figure 2I-K), while IK_{Ca} staining was found in both layers, although expression was stronger in the endothelium (Figure 2E-G). Specificity of the staining for each antibody was confirmed by absence after incubation with the antigenic peptide (Figure 2D, H, L).

Role of Gap Junctions in EDHF Responses

A combination of the gap mimetic peptides (37,43 gap27, 40 gap27 & 43 gap26, 100 μ M each) was used as a pharmacological means of assessing the role of gap junctions in ACh-induced relaxations. In WKY, gap peptides caused a significant rightward shift of the ACh curve, which was not shifted any further by IbTx (Figure 3). In untreated and enalapril-treated SHR, the gap peptides had no effect on responses, although the

addition of IbTx produced a large significant rightward shift of responses in untreated SHR and a smaller significant shift in enalapril-treated rats (Figure 3). In WKY, IbTx administered without gap peptides also produced a significant rightward shift in the dose response curve to ACh (pD₂: -7.5 ± 0.1 , n=4).

Resting membrane potentials did not vary significantly in the gap peptides in any of the rat groups (Table 2; Gap Peptides). However, the hyperpolarisation elicited by ACh (0.1 μ M) was significantly attenuated by the gap peptides in WKY, but not in SHR or SHR+enalapril (Table 2; Figure 4A-F). This concentration of ACh was chosen as it produced a response which was just maximal in all 3 rat groups (see Figure 1).

Role of EETs in EDHF Responses

Due to the involvement of BK_{Ca} channels in EDHF-mediated dilation in all three rat groups (Figure 1), the contribution of EETs was assessed using 14,15-EEZE (10 μ M) (Larsen et al., 2008) and miconazole (1 μ M). ACh responses were significantly shifted to the right in WKY and enalapril-treated SHR, but were not affected in SHR, an effect that was also paralleled by miconazole (Table 3). IbTx had no additional inhibitory effect on responses beyond that seen with EEZE in the two affected groups, but did produce a significant shift in untreated SHR (Table 3). In contrast, the addition of the gap peptide combination failed to produce a further significant rightward shift in any of the rat groups (Table 3).

To rule out the involvement of K_{ATP} channels in the actions of miconazole (1 μ M) and 14,15-EEZE (10 μ M), we tested these compounds on relaxations to levcromakalim in WKY and found no significant reduction due to either of the compounds ($P > 0.05$, n = 4). Glibenclamide also had no significant effect on EDHF dilatations to ACh ($P > 0.05$, n = 4), confirming the lack of involvement of K_{ATP} channels.

The contribution of EETs to ACh-induced hyperpolarisation was assessed using 14,15-EEZE (10 μ M), which had no significant effect on resting membrane potential in any of the rat groups (Table 2). In contrast to the gap peptides, the hyperpolarisation elicited by ACh was attenuated by EEZE in WKY and enalapril-treated SHR, but not in SHR (Table 2; Figure 4G-I).

To determine whether the reactivity to EETs varied amongst the rat groups, we tested the dilatory effects of the four EET regioisomers (5,6-EET, 8,9-EET, 11,12-EET & 14,15-EET; 0.01 – 10 μ M) in endothelium-intact and denuded arteries. We found no significant difference in responsiveness to the EET isomers between endothelium-intact and denuded arteries in any of the rat groups (Figure 5). In addition, there was no significant difference in sensitivity to a particular EET isomer amongst the rat groups, nor any elevated sensitivity to a particular isomer within a rat group.

Role of Hydrogen Peroxide in EDHF Responses

Since hydrogen peroxide has been described as an EDHF which could activate BK_{Ca} channels (Barlow and White, 1998), we incubated arterial segments in catalase (2000 U/ml) in order to investigate the non-EET mediated activation of BK_{Ca} in SHR. However, we found no significant effect on relaxations to ACh in SHR, or in WKY (pD₂ values in catalase, WKY: -7.9 ± 0.1 , n = 4; SHR: -7.9 ± 0.4 , n = 4).

Changes in Morphology within the Arterial Wall amongst Rat Groups

Immunohistochemical staining for Cxs37, 40 and 43 in whole mount preparations showed that gap junctions containing these Cxs were primarily localized to endothelial cell perimeters (Figure 6A-C). No clear staining could be detected for any of the Cxs in the smooth muscle cell layers of whole mount preparations or in transverse sections.

Using Cx40 immunoreactivity, we found that endothelial cells were significantly smaller in arteries from SHR than WKY and that enalapril treatment did not reverse this effect (Table 4). The length and width of endothelial cells did not differ significantly amongst the groups, although the perimeter was significantly smaller in the SHR (Table 4).

As the endothelial cells varied in size, quantification of Cx staining was determined per endothelial cell. Expression of Cx37 was not significantly different between WKY and SHR but was reduced in enalapril-treated SHR (Figure 6D). In contrast, expression of Cxs40 and 43 was significantly reduced in endothelia of arteries from SHR, compared to WKY (Figure 6D). Enalapril treatment did not lead to any significant reversal of these changes (Figure 6D).

Electron microscopic analysis showed that arteries from SHR had significantly more smooth muscle cell layers than those from WKY, although vessel diameter was not significantly different amongst the experimental groups (Table 5). Enalapril treatment of SHR did not produce any significant reduction in the number of layers (Table 5).

Both the number of MEGJs containing pentalaminar membrane (Figure 7A, B) and the number of potential MEGJs (Figure 7C, D) were significantly reduced in SHR compared with WKY and this was not altered by treatment with enalapril (Table 5). Projections from one cell layer to the other were not counted as potential MEGJs if there was a clear gap between the cell membranes (Figure 7E). Pentalaminar gap junctions were readily found between adjacent endothelial cells (Figure 7F).

Since MEGJs form on projections of either endothelial or smooth muscle cells which penetrate the IEL (Sandow and Hill, 2000), counts were made of the number of holes in the IEL and expressed per endothelial cell using the data in Table 4.

Significantly fewer holes were found in arteries from SHR and enalapril-treated SHR than in arteries from WKY (Table 6). Punctate staining for IK_{Ca} channels and for IP_3R1 , which were used as markers for myoendothelial projections, was detected within some of the holes in the IEL, above the level of the endothelium (Figure 8A-D, G).

Comparable staining for IP_3R2 was also found while IP_3R3 was less prevalent at this level (Figure 8E, F). When expressed per endothelial cell, the number of holes showing staining for either IK_{Ca} channels or IP_3R1 in SHR or enalapril-treated SHR was significantly less than that seen in WKY ($P < 0.05$, one-way ANOVA; Table 6).

Furthermore, in each rat group, the number of holes showing staining for either IK_{Ca} channels or IP_3R1 was significantly less than the total number of holes ($P < 0.05$, one-way ANOVA; Table 6) and significantly less than the total number of MEGJs, including the potential MEGJs ($P < 0.05$, one-way ANOVA; Tables 5 and 6). The total number of MEGJs per endothelial cell was in turn significantly less than the total number of holes in the IEL per endothelial cell in each group ($P < 0.05$, unpaired t-test; Tables 5 and 6, respectively).

Discussion

Heterogeneous mechanisms underlie EDHF responses in small mesenteric arteries of aged SHR and WKY rats. In WKY, EDHF-mediated relaxation comprised gap junction and EET-dependent mechanisms, while in SHR, gap junction independent mechanisms prevailed, with a prominent role for EET- and hydrogen peroxide-independent BK_{Ca} channel activity. Significant morphological changes were also apparent in SHR, with increase in smooth muscle cell layers, but reduction in the size of endothelial cells and coupling both within the endothelium and between the endothelium and smooth muscle via MEGJs. Treatment of SHR with the angiotensin

converting enzyme inhibitor, enalapril, decreased blood pressure and restored an EET component to the dilation, but failed to reverse morphological changes or restore cell coupling and gap peptide sensitivity of EDHF responses.

ACh produced substantial hyperpolarisation of smooth muscle cells in all rat groups and our previous studies showed these responses arise in the endothelium (Goto et al., 2004b). However, the amplitude of hyperpolarisation was 30% smaller in SHR than in WKY, but restored by enalapril. This reduction was not due to an inability of the endothelium or smooth muscle to hyperpolarize, since neither hyperpolarisation nor relaxation evoked by K channel openers was affected. The absence of any consistent reduction in ACh-induced relaxation in SHR may be due to the measurement of relaxation as reversal of phenylephrine-induced tone which produced only 10mV depolarization, while ACh-induced hyperpolarisations were greater than 20mV (Table 1). However, the reduced hyperpolarisation in SHR may heighten sensitivity to K_{Ca} inhibitors.

Serial section electron microscopy revealed fewer MEGJs per endothelial cell in mesenteric arteries of SHR than WKY and fewer holes in the IEL through which endothelial cells project; neither parameter being reversed by enalapril treatment. The incidence of IK_{Ca} channels in the IEL, which reflects the presence of MEGJs (Sandow et al., 2006), was similarly reduced. IP_3R1 , $R2$ and, to a lesser extent, $R3$ receptors, were also found in the same location and their incidence mirrored the changes occurring in MEGJs, suggesting that all three structures are located in endothelial projections. The IP_3 pathway was previously shown to be essential to muscarinic receptor signalling in mesenteric arteries (Goto et al., 2007). The reduced MEGJ coupling is unlikely restricted by the IEL holes in SHR and enalapril-treated SHR arteries, as the number of holes still outnumbered the number of MEGJs by 3-4 fold. Together with the

insensitivity to gap peptides of ACh relaxations in SHR and enalapril-treated SHR, the data show that MEGJs in these arteries do not influence EDHF-mediated vasodilation.

Gap junctions comprised of Cxs 40 and 43, but not Cx37, were also decreased in the endothelium of SHR arteries and, like MEGJs, were not changed by enalapril treatment. Previous studies in large, elastic, superior mesenteric arteries of SHR also described decreases in endothelial Cxs and associated these changes with diminished EDHF responses, both being reversed by candesartan treatment (Kansui et al., 2004). A causal link between EDHF and endothelial Cx expression in these arteries was also made following chronic treatment with angiotensin II (Dal-Ros et al., 2009). In contrast, we found no association between reduced endothelial Cxs40 and 43 and EDHF relaxation in the downstream muscular branches of the superior mesenteric artery. Furthermore, while ACh-induced hyperpolarisations in SHR were restored by enalapril, the alterations to Cxs persisted. Although longer treatments might have reversed changes in endothelial Cx expression, since a trend to reversal was noted with Cx40, the data highlight a dissociation between the effects of the renin-angiotensin system on Cx expression and EDHF-mediated hyperpolarisation, and point to differences in the regulation of EDHF in large, elastic compared to smaller, muscular arteries.

The absence of change to Cx37 expression in SHR arteries suggests a diminishing relationship between hypertension and this Cx with age. Previous studies have shown 25% less Cx37 in muscular mesenteric arteries of SHR than WKY at 3 months of age (Goto et al., 2004b), while this difference was less than 10% at 8 months of age. While changes in endothelial Cxs were reversed following blockade of the renin-angiotensin system in mesenteric and caudal arteries in younger SHR (Kansui et al., 2004; Rummery et al., 2005), the absence of changes in aged SHR suggests a developing insensitivity of Cx expression in established hypertension.

Our functional data revealed a role for EETs in EDHF-mediated vasodilatory responses of WKY, but not SHR. EETs are catabolised by soluble epoxide hydrolase, whose expression is upregulated by angiotensin II (Ai et al., 2007). Thus, when angiotensin II levels are elevated in SHR, soluble epoxide hydrolase is upregulated and EETs reduced (Yu et al., 2000). Consistent with this, ACh-evoked hyperpolarisations and dilations in SHR were insensitive to the EET antagonist, 14,15-EEZE, while responses in enalapril-treated SHR displayed a 'restoration' of sensitivity to EEZE – an effect paralleled by the cytochrome P450 inhibitor, miconazole. Experiments using the four EET regioisomers demonstrated that despite elevated EET catabolism, the SHR arteries are capable of relaxing to exogenously applied EETs and do so independently of the endothelium. While these experiments may suggest that alterations in circulating angiotensin II levels can influence the mechanisms recruited to elicit EDHF, we cannot rule out the possibility that other anti-hypertensive therapies, which do not directly alter angiotensin II levels, could restore a role for EETs simply through their blood pressure lowering effects.

The involvement of EETs in EDHF mechanisms in the rat mesenteric artery has previously been excluded since sensitivity to cytochrome P450 inhibitors, like miconazole, could be explained by non-specific inhibition of K_{ATP} channels (Vanheel and Van de Voorde, 1997). However, EDHF relaxations to ACh in our study were insensitive to the K_{ATP} channel blocker glibenclamide and relaxations to the K_{ATP} channel opener levcromakalim were not affected by miconazole. It is also unlikely that the selective effect of miconazole in WKY, but not SHR arteries, could be attributed to differential K_{ATP} activity since we found no differences in responses to levcromakalim between these rat groups. Indeed, the similarities in effects of 14,15-EEZE with those

of miconazole lends strong support to the idea that EETs contribute to EDHF in our preparation.

EETs act primarily through BK_{Ca} channels (Larsen et al., 2008) via G-protein-dependent mechanisms (Li and Campbell, 1997). Lack of any further effect of IbTx over 14,15-EEZE in WKY and enalapril-treated SHR, supports an action of EETs via BK_{Ca} channels; BK_{Ca} channel involvement in EDHF was prominent in all groups after SK_{Ca} and IK_{Ca} channel blockade. Staining confirmed that BK_{Ca} channels were confined to the smooth muscle layers of arteries in all rats, consistent with the site of action of the EET regioisomers. In contrast, SK_{Ca} channels were only in the endothelium while IK_{Ca} channels were in both endothelium and smooth muscle cell layers. We speculate that overlapping effects of EEZE, IbTx and gap peptides in WKY might indicate an action of EETs on endothelial TRPV4 channels, and transfer of calcium through MEGJs into smooth muscle cells to activate BK_{Ca} channels (Loot et al., 2008). Absence of a gap junction component to the ACh response in enalapril-treated SHR suggests that different mechanisms underlie EET actions in the two rat groups, posing tantalizing questions for future studies.

In SHR the addition of IbTx had a substantial inhibitory effect on dilation, although the mediator remains unclear as neither EETs nor hydrogen peroxide were involved. An EET-independent BK_{Ca} component to EDHF has also been described in the mouse microcirculation (Siegl et al., 2005). Alterations in activity and expression of BK_{Ca} channels are well documented during hypertension (Kamouchi et al., 2002) and may arise as a means to offset enhanced vasomotor tone. The attenuation of IbTx sensitivity by enalapril in SHR is consistent with the reported effects of ramipril on K_{Ca} and K_V currents in SHR myocytes (Cox et al., 2002).

We found hypertrophic remodeling of the arterial wall in aged SHR similar to that reported in primary and secondary mesenteric branches of younger rats (Inoue et al., 1990; Yang et al., 2004), but in contrast to eutrophic remodeling of tertiary branches (Intengan et al., 1999). Such variations likely relate to differential pressures exerted in vessels of different size throughout the mesenteric bed (Fenger-Gron et al., 1995). As with gap junctions, enalapril treatment did not reverse hypertrophic remodeling in SHR, consistent with the effect of quinapril on secondary mesenteric branches, although a longer treatment did show significant reductions in muscle layers (Yang et al., 2004). The absence of an effect of enalapril on the decrease in endothelial cell size seen in SHR arteries in the present study is consistent with our previous work in mesenteric and caudal arteries of younger SHR (Rummery et al., 2002; Goto et al., 2004b; Rummery et al., 2005).

In summary, ACh can evoke comparable EDHF-mediated relaxations in muscular mesenteric arteries from aged normotensive and angiotensin II-dependent hypertensive rats, albeit through different mechanisms. In WKY, relaxations are gap junction- and EET-dependent, while in SHR, EDHF persists in the absence of myoendothelial coupling, through the increased importance of BK_{Ca} channels, independently of EETs or hydrogen peroxide. Reduction in blood pressure through inhibition of the renin-angiotensin system restored a role for EETs without gap junctional involvement or other morphological alterations. Thus, robust EDHF-mediated responses can be evoked in the absence of myoendothelial coupling, and it is possible that circulating angiotensin II can influence the mechanisms recruited to elicit EDHF dilation.

References

- Ai D, Fu Y, Guo D, Tanaka H, Wang N, Tang C, Hammock BD, Shyy JY and Zhu Y (2007) Angiotensin II up-regulates soluble epoxide hydrolase in vascular endothelium in vitro and in vivo. *Proc Natl Acad Sci U S A* **104**:9018-9023.
- Barlow RS and White RE (1998) Hydrogen peroxide relaxes porcine coronary arteries by stimulating BKCa channel activity. *Am J Physiol* **275**:H1283-1289.
- Chaytor AT, Evans WH and Griffith TM (1997) Peptides homologous to extracellular loop motifs of connexin 43 reversibly abolish rhythmic contractile activity in rabbit arteries. *J Physiol* **503** (Pt 1):99-110.
- Cox RH, Lozinskaya I, Matsuda K and Dietz NJ (2002) Ramipril treatment alters Ca(2+) and K(+) channels in small mesenteric arteries from Wistar-Kyoto and spontaneously hypertensive rats. *Am J Hypertens* **15**:879-890.
- Dal-Ros S, Bronner C, Schott C, Kane MO, Chataigneau M, Schini-Kerth VB and Chataigneau T (2009) Angiotensin II-induced hypertension is associated with a selective inhibition of endothelium-derived hyperpolarizing factor-mediated responses in the rat mesenteric artery. *J Pharmacol Exp Ther* **328**:478-486.
- Feletou M and Vanhoutte PM (2006) Endothelium-derived hyperpolarizing factor: where are we now? *Arterioscler Thromb Vasc Biol* **26**:1215-1225.
- Fenger-Gron J, Mulvany MJ and Christensen KL (1995) Mesenteric blood pressure profile of conscious, freely moving rats. *J Physiol* **488**:753-760.
- Goto K, Edwards FR and Hill CE (2007) Depolarization evoked by acetylcholine in mesenteric arteries of hypertensive rats attenuates endothelium-dependent hyperpolarizing factor. *J Hypertens* **25**:345-359.
- Goto K, Fujii K, Kansui Y and Iida M (2004a) Changes in endothelium-derived hyperpolarizing factor in hypertension and ageing: response to chronic treatment

with renin-angiotensin system inhibitors. *Clin Exp Pharmacol Physiol* **31**:650-655.

Goto K, Fujii K, Onaka U, Abe I and Fujishima M (2000) Renin-angiotensin system blockade improves endothelial dysfunction in hypertension. *Hypertension* **36**:575-580.

Goto K, Rummery NM, Grayson TH and Hill CE (2004b) Attenuation of conducted vasodilatation in rat mesenteric arteries during hypertension: role of inwardly rectifying potassium channels. *J Physiol* **561**:215-231.

Grayson TH, Haddock RE, Murray TP, Wojcikiewicz RJ and Hill CE (2004) Inositol 1,4,5-trisphosphate receptor subtypes are differentially distributed between smooth muscle and endothelial layers of rat arteries. *Cell Calcium* **36**:447-458.

Griffith TM, Chaytor AT and Edwards DH (2004) The obligatory link: role of gap junctional communication in endothelium-dependent smooth muscle hyperpolarization. *Pharmacol Res* **49**:551-564.

Inoue T, Masuda T and Kishi K (1990) Structural and functional alterations of mesenteric vascular beds in spontaneously hypertensive rats. *Jpn Heart J* **31**:393-403.

Intengan HD, Thibault G, Li JS and Schiffrin EL (1999) Resistance artery mechanics, structure, and extracellular components in spontaneously hypertensive rats : effects of angiotensin receptor antagonism and converting enzyme inhibition. *Circulation* **100**:2267-2275.

Isakson BE, Ramos SI and Duling BR (2007) Ca²⁺ and inositol 1,4,5-trisphosphate-mediated signaling across the myoendothelial junction. *Circ Res* **100**:246-254.

- Kamouchi M, Kitazono T, Nagao T, Fujishima M and Ibayashi S (2002) Role of CA(2+)-activated K⁺ channels in the regulation of basilar arterial tone in spontaneously hypertensive rats. *Clin Exp Pharmacol Physiol* **29**:575-581.
- Kansui Y, Fujii K, Nakamura K, Goto K, Oniki H, Abe I, Shibata Y and Iida M (2004) Angiotensin II receptor blockade corrects altered expression of gap junctions in vascular endothelial cells from hypertensive rats. *Am J Physiol Heart Circ Physiol* **287**:H216-224.
- Larsen BT, Gutterman DD, Sato A, Toyama K, Campbell WB, Zeldin DC, Manthati VL, Falck JR and Miura H (2008) Hydrogen peroxide inhibits cytochrome p450 epoxygenases: interaction between two endothelium-derived hyperpolarizing factors. *Circ Res* **102**:59-67.
- Li PL and Campbell WB (1997) Epoxyeicosatrienoic acids activate K⁺ channels in coronary smooth muscle through a guanine nucleotide binding protein. *Circ Res* **80**:877-884.
- Loot AE, Popp R, Fisslthaler B, Vriens J, Nilius B and Fleming I (2008) Role of cytochrome P450-dependent transient receptor potential V4 activation in flow-induced vasodilatation. *Cardiovasc Res* **80**:445-452.
- Matchkov VV, Rahman A, Bakker LM, Griffith TM, Nilsson H and Aalkjaer C (2006) Analysis of effects of connexin-mimetic peptides in rat mesenteric small arteries. *Am J Physiol Heart Circ Physiol* **291**:H357-367.
- Mather S, Dora KA, Sandow SL, Winter P and Garland CJ (2005) Rapid endothelial cell-selective loading of connexin 40 antibody blocks endothelium-derived hyperpolarizing factor dilation in rat small mesenteric arteries. *Circ Res* **97**:399-407.

- Neylon CB, Nurgali K, Hunne B, Robbins HL, Moore S, Chen MX and Furness JB (2004) Intermediate-conductance calcium-activated potassium channels in enteric neurones of the mouse: pharmacological, molecular and immunochemical evidence for their role in mediating the slow afterhyperpolarization. *J Neurochem* **90**:1414-1422.
- Rummery NM, Grayson TH and Hill CE (2005) Angiotensin-converting enzyme inhibition restores endothelial but not medial connexin expression in hypertensive rats. *J Hypertens* **23**:317-328.
- Rummery NM, McKenzie KU, Whitworth JA and Hill CE (2002) Decreased endothelial size and connexin expression in rat caudal arteries during hypertension. *J Hypertens* **20**:247-253.
- Sadow SL, Bramich NJ, Bandi HP, Rummery NM and Hill CE (2003) Structure, function, and endothelium-derived hyperpolarizing factor in the caudal artery of the SHR and WKY rat. *Arterioscler Thromb Vasc Biol* **23**:822-828.
- Sadow SL, Goto K, Rummery NM and Hill CE (2004) Developmental changes in myoendothelial gap junction mediated vasodilator activity in the rat saphenous artery. *J Physiol* **556**:875-886.
- Sadow SL and Hill CE (2000) Incidence of myoendothelial gap junctions in the proximal and distal mesenteric arteries of the rat is suggestive of a role in endothelium-derived hyperpolarizing factor-mediated responses. *Circ Res* **86**:341-346.
- Sadow SL, Neylon CB, Chen MX and Garland CJ (2006) Spatial separation of endothelial small- and intermediate-conductance calcium-activated potassium channels (K(Ca)) and connexins: possible relationship to vasodilator function? *J Anat* **209**:689-698.

- Sandow SL, Tare M, Coleman HA, Hill CE and Parkington HC (2002) Involvement of myoendothelial gap junctions in the actions of endothelium-derived hyperpolarizing factor. *Circ Res* **90**:1108-1113.
- Siegl D, Koeppen M, Wolfle SE, Pohl U and de Wit C (2005) Myoendothelial coupling is not prominent in arterioles within the mouse cremaster microcirculation in vivo. *Circ Res* **97**:781-788.
- Tare M, Coleman HA and Parkington HC (2002) Glycyrrhetic derivatives inhibit hyperpolarization in endothelial cells of guinea pig and rat arteries. *Am J Physiol Heart Circ Physiol* **282**:H335-341.
- Triggle CR, Hollenberg M, Anderson TJ, Ding H, Jiang Y, Ceroni L, Wiehler WB, Ng ES, Ellis A, Andrews K, McGuire JJ and Pannirselvam M (2003) The endothelium in health and disease--a target for therapeutic intervention. *J Smooth Muscle Res* **39**:249-267.
- Vanheel B and Van de Voorde J (1997) Evidence against the involvement of cytochrome P450 metabolites in endothelium-dependent hyperpolarization of the rat main mesenteric artery. *J Physiol* **501**:331-341.
- Wojcikiewicz RJ (1995) Type I, II, and III inositol 1,4,5-trisphosphate receptors are unequally susceptible to down-regulation and are expressed in markedly different proportions in different cell types. *J Biol Chem* **270**:11678-11683.
- Yang L, Gao YJ and Lee RM (2004) Quinapril effects on resistance artery structure and function in hypertension. *Naunyn Schmiedebergs Arch Pharmacol* **370**:444-451.
- Yang Z and Kaye DM (2006) Endothelial dysfunction and impaired L-arginine transport in hypertension and genetically predisposed normotensive subjects. *Trends Cardiovasc Med* **16**:118-124.

Yu Z, Xu F, Huse LM, Morisseau C, Draper AJ, Newman JW, Parker C, Graham L, Engler MM, Hammock BD, Zeldin DC and Kroetz DL (2000) Soluble epoxide hydrolase regulates hydrolysis of vasoactive epoxyeicosatrienoic acids. *Circ Res* **87**:992-998.

Zhang DX, Mendoza SA, Bubolz AH, Mizuno A, Ge ZD, Li R, Warltier DC, Suzuki M and Gutterman DD (2009) Transient receptor potential vanilloid type 4-deficient mice exhibit impaired endothelium-dependent relaxation induced by acetylcholine in vitro and in vivo. *Hypertension* **53**:532-538.

Footnotes

AE and KG contributed equally to this study which was supported by grants from the National Heart Foundation [G03C1059 to CEH]; National Health and Medical Research Council of Australia [224219 to CEH]; National Institutes of Health [DK49194 to RJHW].

Present address for Dr Goto: Department of Medicine and Clinical Science, Graduate School of Medical Sciences, Kyushu University, Maidashi 3-1-1, Higashi-ku, Fukuoka 812-8582, Japan

Legends for Figures

Figure 1: Role of calcium activated potassium channels in EDHF responses. ACh-induced dilations in mesenteric artery from WKY, SHR and enalapril-treated SHR (SHRe) were significantly attenuated by apamin (500 nM), TRAM-34 (500 nM), ODQ (10 μ M) and iberiotoxin (500 nM). Data expressed as % reversal of a submaximal phenylephrine-induced tone (0.3 – 1 μ M). Points represent means and SEM. *** $P < 0.001$, when compared to respective controls, two-way ANOVA.

Figure 2: Calcium dependent potassium channel expression in mesenteric arteries from WKY, SHR and enalapril-treated SHR. A-C. SK_{Ca} expression was confined to the endothelium in WKY (A), SHR (B) and enalapril-treated SHR (C). E-G. IK_{Ca} expression was found in both endothelium and smooth muscle of WKY (E), SHR (F) and enalapril-treated SHR (G). I-K. BK_{Ca} expression was confined to the smooth muscle of WKY (I), SHR (J) and enalapril-treated SHR (K). Staining for each antibody was eliminated by preincubation with the immunizing peptide (D SK_{Ca}; H IK_{Ca}; L BK_{Ca}).

Figure 3: Effect of gap mimetic peptides (^{37,43}gap 27, ⁴⁰gap 27, ⁴³gap 26, GP 100 μ M of each) and iberiotoxin (IbTx 100 nM) on EDHF responses. Gap peptides attenuated ACh-induced dilations only in arteries from WKY ($P < 0.001$, compared to control, $n = 7$). IbTx substantially reduced dilations in SHR ($P < 0.001$, $n = 7$) but less so in enalapril-treated SHR ($P < 0.05$, $n = 5$). Data expressed as % reversal of a submaximal phenylephrine-induced tone (0.3 – 1 μ M). Points represent means and SEM.

Figure 4: Effect of gap peptides and EEZE on hyperpolarisations to ACh.

Hyperpolarisation induced by ACh (0.1 μ M) under control conditions in mesenteric arterial segments taken from WKY (A), SHR (B) and enalapril-treated SHR (C) and after incubation in gap mimetic peptides (^{37,43}gap 27, ⁴⁰gap 27, ⁴³gap 26 GP 100 μ M of each) in WKY (D), SHR (E) and enalapril-treated SHR (F). Effects of incubation in EEZE (10 μ M) on responses in WKY, SHR and enalapril-treated SHR are shown in G-I, respectively. Note the decreased amplitude of responses in D, G and I compared with the control response in the same rat group.

Figure 5: Dilations to epoxyeicosatrienoic acid (EET) regioisomers in endothelium-intact and denuded mesenteric arteries from WKY (n =4), SHR (n =4) and enalapril-treated SHR (n =4). All rat groups dilated to EETs with no significant difference between endothelium-intact and denuded arteries. Data expressed as % reversal of a submaximal phenylephrine-induced tone (0.3 – 1 μ M). Points represent means and SEM.

Figure 6: Connexin expression in the endothelium of mesenteric arteries.

Immunohistochemistry using antibodies against Cxs37 (A), 40 (B) and 43 (C) showed that gap junctions containing these Cxs were primarily localized to endothelial cell perimeters in all rat groups (arrows; WKY). Quantification was undertaken using ImageJ, taking into account the endothelial cells sizes presented in Table 3. Data represents means and standard errors of means for preparations taken from 3-4 rats. * $P < 0.05$, when compared to WKY of the corresponding Cx group.

Figure 7: A. Typical MEGJ formed at the end of an endothelial cell (ec) projection through the internal elastic lamina (iel). Dotted lines represent the focal planes of optical confocal sections shown in panels A, B and C of Figure 8. B. Pentalaminar membrane at point of contact between endothelial cell and smooth muscle cell (smc) in A (arrows, box). C, D. Possible MEGJs at which there is no detectable gap between smooth muscle and endothelial membranes (arrows). E. Endothelial projection with gap between the cell membranes would not be counted as a MEGJ. F. Endothelial gap junction with pentalaminar membrane (arrow). Calibration bars represent 20 μm in A, C, E, 10 μm in D and F and 1 μm in B.

Figure 8: Immunohistochemical staining for IP₃R1 (A-D), IP₃R2 (E), IP₃R3 (F) receptors and IK_{Ca} channels (G) within the holes of the internal elastic lamina of mesenteric arteries from WKY rats. A. Staining for IP₃R1 (red) in optical confocal sections taken through the holes of the internal elastic lamina (green), at the level depicted by the dotted line marked AB in Figure 7A. B. same field showing only the IP₃R1 staining (red) which lies in this focal plane, above the level of the endothelial cell layer (not in focus). C. same field showing only the IP₃R1 staining (blue) present in the focal plane through the endothelial cell layer, as shown by the dotted line marked C in Figure 7A. D. same field with the IP₃R1 staining in the holes (red) superimposed on the IP₃R1 staining in the endothelial cell layer (blue). Note that the staining in the holes of the internal elastic lamina is not seen in the same focal plane as the staining in the endothelial cell layer (compare arrows in panels B and C with D). Note also that some of the staining lying in a diagonal line above the lower 3 arrows in Panel B is actually at the level of the endothelial cell layer, due to the uneven nature of the whole mount preparations and hence represents false positives. E-G. Similar staining exists within

holes of the internal elastic lamina (arrows) in the case of IP₃R2 (E), IP₃R3 (F) receptors and IK_{Ca} channels (G). Longitudinal axis of the vessel runs top to bottom of each panel.

Bars represent 10 μm.

Tables

Table 1. Resting Membrane Potential Measurements (RMP) in Control and in Acetylcholine (ACh) in the Presence and Absence of Phenylephrine.

	WKY	SHR	SHR+enalapril
Without phenylephrine			
RMP	-52 ± 0.4 mV (8)	-49 ± 0.9 mV (10)	-51 ± 0.9 mV (10)
RMP in ACh (1 μM)	-72 ± 1.0 mV (7)	-62 ± 1.6 mV (6)*	-69 ± 1.3 mV (6)
With phenylephrine (1 μM)			
RMP	-39 ± 0.9 mV (8)	-40 ± 0.7 mV (8)	-41 ± 0.7 mV (7)
RMP in ACh (1 μM)	-69 ± 1.3 mV (6)	-60 ± 1.5 mV (6)*	-70 ± 1.7 mV (5)

* $P < 0.05$, when compared to WKY or SHR-enalapril, one way ANOVA; Mean ± SEM. Numbers in parentheses represent number of rats.

Table 2. Resting Membrane Potential Measurements (RMP) in Control and in Acetylcholine (ACh) in the Presence and Absence of antagonists against EETs (EEZE) and Gap Junctions (gap peptides).

	WKY	SHR	SHR+enalapril
Control			
RMP	-50 ± 0.4 mV (11)	-48 ± 0.5 mV (5)	-50 ± 1.1 mV (4)
RMP in ACh (0.1 μM)	-71 ± 0.6 mV (11)	-63 ± 2.1 mV (5) [†]	-72 ± 1.7 mV (4)
Gap Peptides			
RMP	-50 ± 1.7 mV (4)	-48 ± 0.9 mV (4)	-49 ± 1.5 mV (3)
RMP in ACh (0.1 μM)	-64 ± 1.5 mV (4)*	-64 ± 0.6 mV (3)	-69 ± 0.3 mV (3)
EEZE			
RMP	-49 ± 1.2 mV (5)	-51 ± 1.4 mV (4)	-50 ± 1.4 mV (4)
RMP in ACh (0.1 μM)	-63 ± 2.4 mV (4)*	-68 ± 3.9 mV (3)	-65 ± 2.2 mV (4)*

[†]*P* < 0.05, when compared to WKY or SHR-enalapril, one way ANOVA;

**P* < 0.05, when compared to control of the same rat group, one way ANOVA;

Mean ± SEM. Numbers in parentheses represent number of rats.

Table 3. Role of epoxyeicosatrienoic acids (EETs) on EDHF-mediated relaxation.

	WKY	SHR	SHR+enalapril
Control	-8.0 ± 0.1 (11)	-7.9 ± 0.1 (9)	-7.9 ± 0.2 (8)
EEZE	-7.4 ± 0.1 (5)*	-8.0 ± 0.1 (5)	-7.2 ± 0.2 (4)*
EEZE/IbTx	-7.3 ± 0.2 (5)*	-7.2 ± 0.1*(5)	-7.1 ± 0.2 (4)*
EEZE/IbTx/GP	-7.1 ± 0.1 (5)*	-7.4 ± 0.2 (5)	-7.1 ± 0.1 (4)*
Miconazole	-7.3 ± 0.1 (4)*	-7.7 ± 0.3 (4)	-7.2 ± 0.1 (3)*

The effects of the EETs antagonist EEZE (10 μM), the BKCa channel inhibitor IbTx (100 nM) and the cytochrome P450 inhibitor miconazole (1 μM) were tested on ACh-induced relaxations of mesenteric arteries taken from WKY, SHR and enalapril-treated SHR. Data summarized as pD₂ values. * P < 0.05, when compared to control of the same rat group, one-way ANOVA. Numbers in parentheses represent number of rats.

Table 4. Morphology of Endothelial Cells

Group	Area (μm^2)	Perimeter (μm)	Length (μm)	Width (μm)
WKY	371 \pm 30 (6; 250)	116 \pm 8	52 \pm 4	12 \pm 1
SHR	287 \pm 27* (4; 160)	100 \pm 8*	46 \pm 4	10 \pm 1
SHR+ enalapril	325 \pm 31* (3; 75)	107 \pm 11	48 \pm 5	11 \pm 1

* $P < 0.05$ compared to WKY. Means and SEM. Number of animals and total number of cells in parentheses.

Table 5. MEGJs and Morphology of the Arterial Wall

Group	Number of SMC layers	Vessel Diameter (μm)	Number of MEGJs per EC	Potential MEGJs per EC
WKY	4.3 \pm 0.3 (5)	205 \pm 11 (5)	0.20 \pm 0.05 (4)	1.68 \pm 0.37 (4)
SHR	6.5 \pm 0.3* (8)	228 \pm 16 (8)	0.05 \pm 0.03* (4)	0.59 \pm 0.05* (4)
SHR+ enalapril	5.8 \pm 0.2* (9)	186 \pm 15 (9)	0.08 \pm 0.03 (4)	0.67 \pm 0.11* (4)

* $P < 0.05$ compared to WKY. Means and SEM with number of animals in parentheses.

SMC smooth muscle cell; EC endothelial cell; IEL internal elastic lamina.

Table 6. IK_{Ca} and IP_3R1 Immunoreactivity at the Internal Elastic Lamina

Group	Number		IK_{Ca}		IP_3R1	
	of holes in IEL per $10^4\mu m^2$	of holes in IEL per EC	Number of holes with staining in IEL per $10^4\mu m^2$	Number of holes with staining in IEL per EC	Number of holes with staining in IEL per $10^4\mu m^2$	Number of holes with staining in IEL per EC
WKY	117±5 (43)	4.3±0.2 (43)	13±1 (12)	0.5±0.1 (12)	15±3 (10)	0.6±0.1 (10)
SHR	69±6* (38)	2.0±0.2* (38)	5±1* (12)	0.1±0.0* (12)	7±1* (9)	0.2±0.0* (9)
SHR+ enalapril	73±9* (38)	2.4±0.3* (38)	7.5±3 (4)	0.2±0.1* (4)	7±1* (6)	0.2±0.0* (6)

* $P < 0.05$ compared to WKY. Means and SEM with number of fields counted in parentheses. Data for number of holes (fenestrations) in IEL is from 7, 6 and 6 animals, respectively. Data for IK_{Ca} and IP_3R1 staining is from 3-4 animals for each group. EC endothelial cell; IEL internal elastic lamina

Figure 1

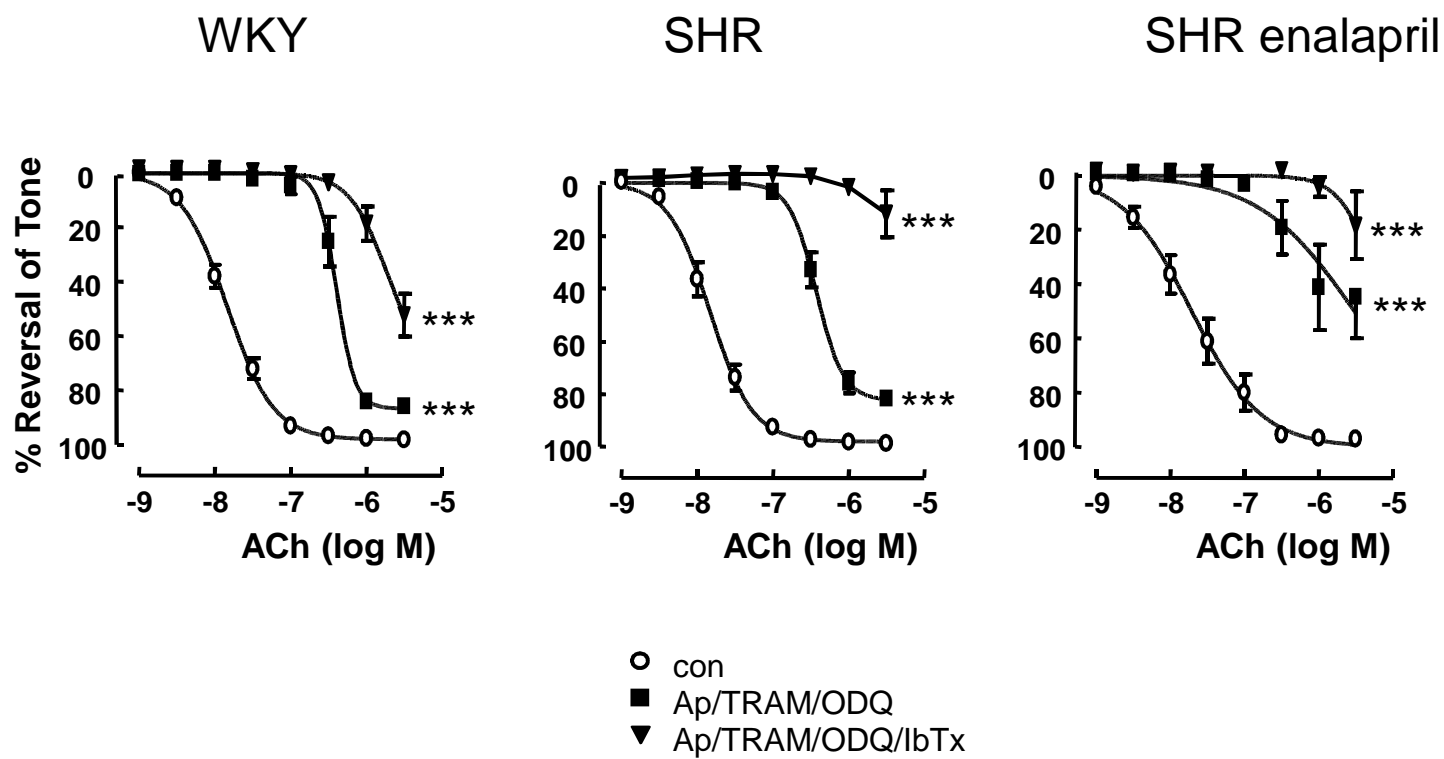


Figure 2

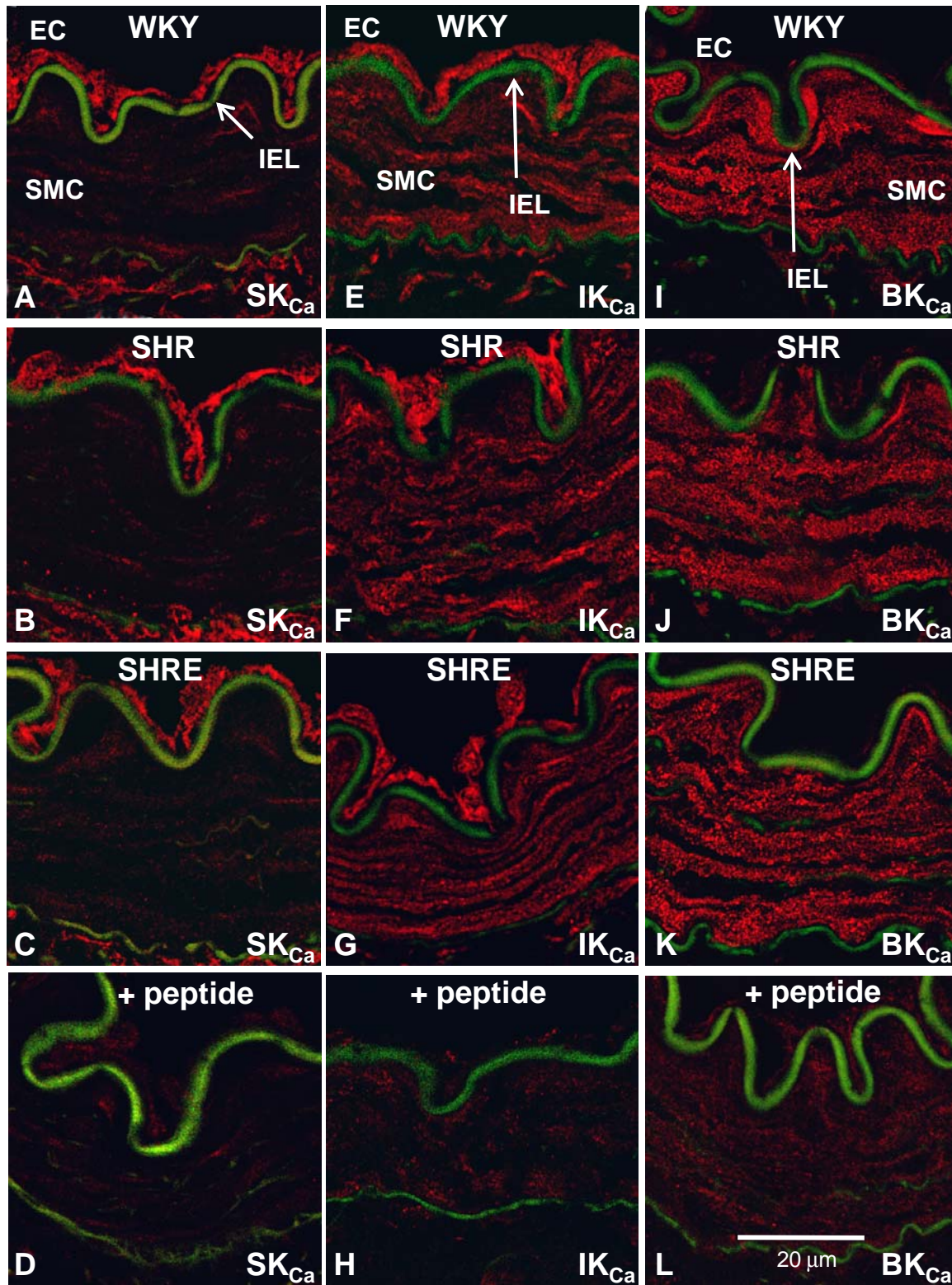


Figure 3

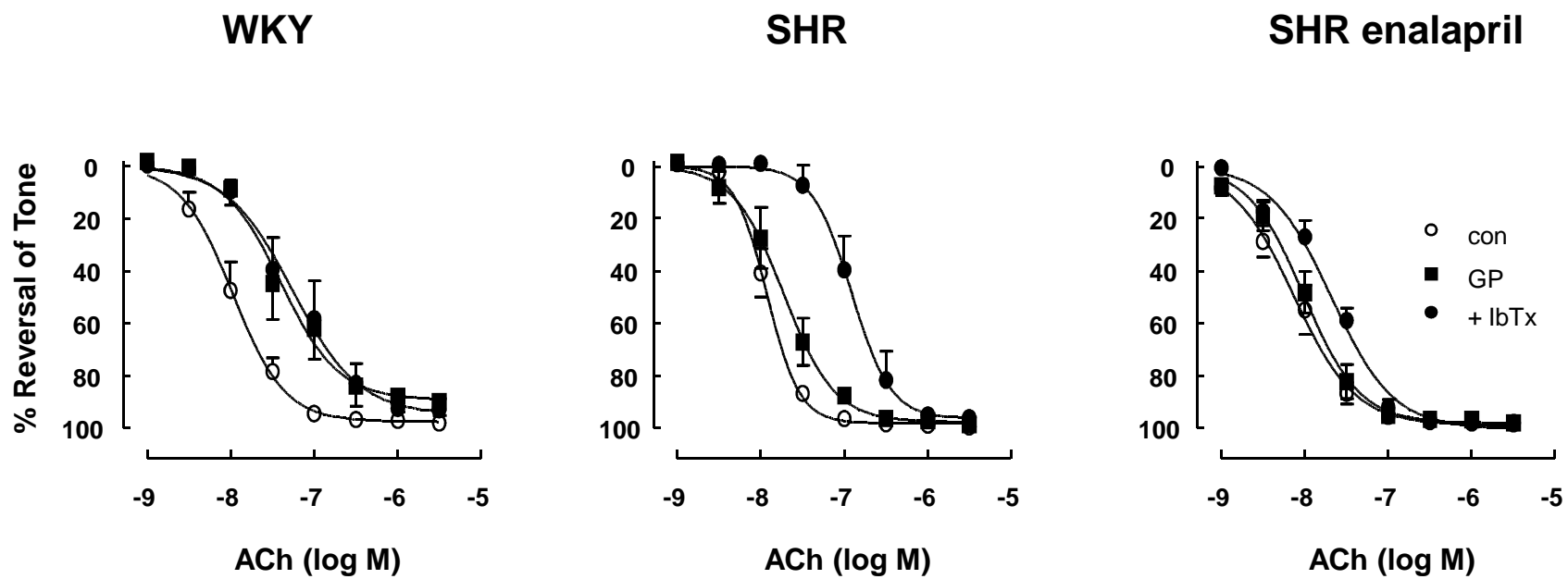


Figure 4

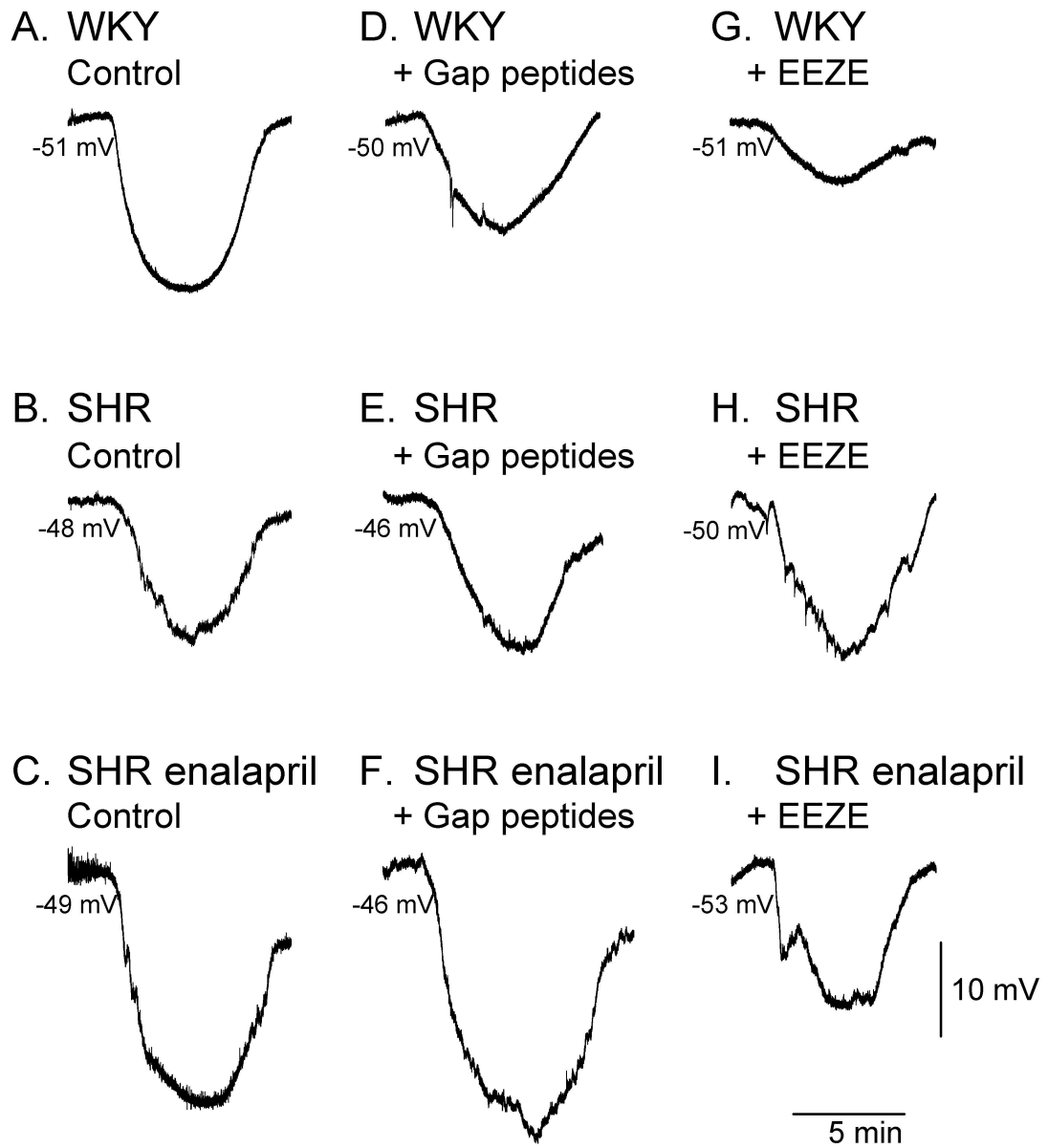


Figure 5

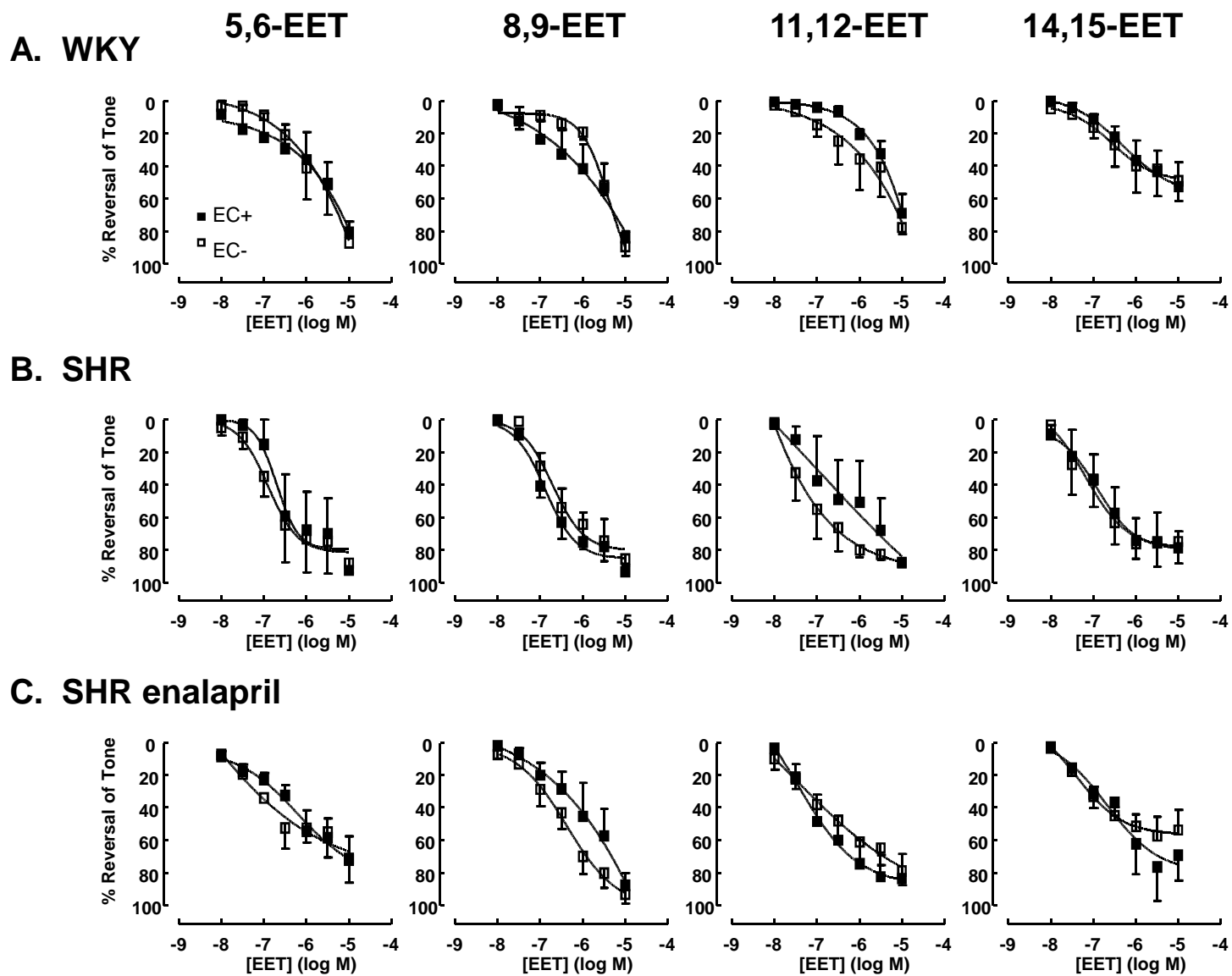


Figure 6

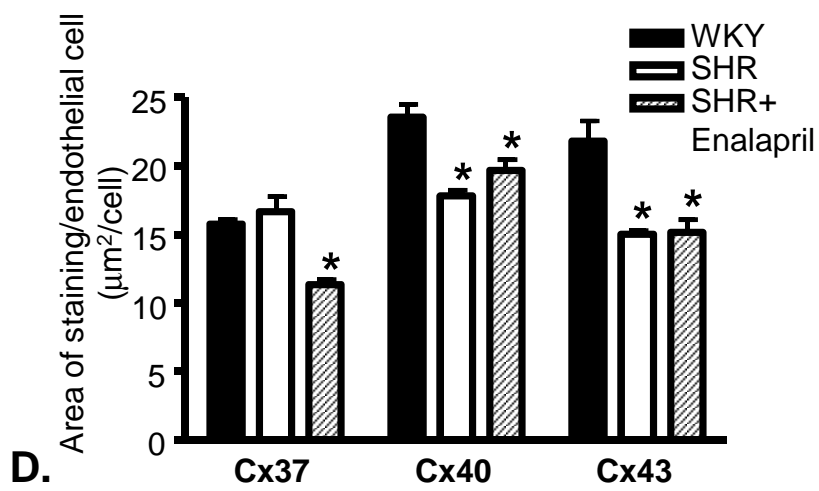
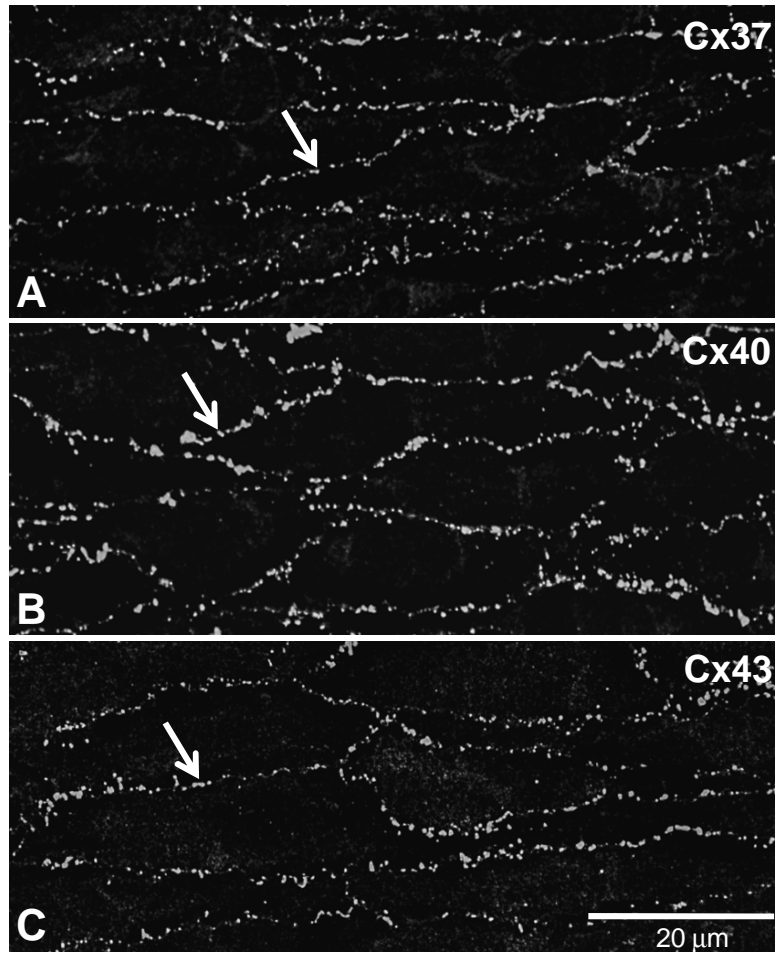


Figure 7

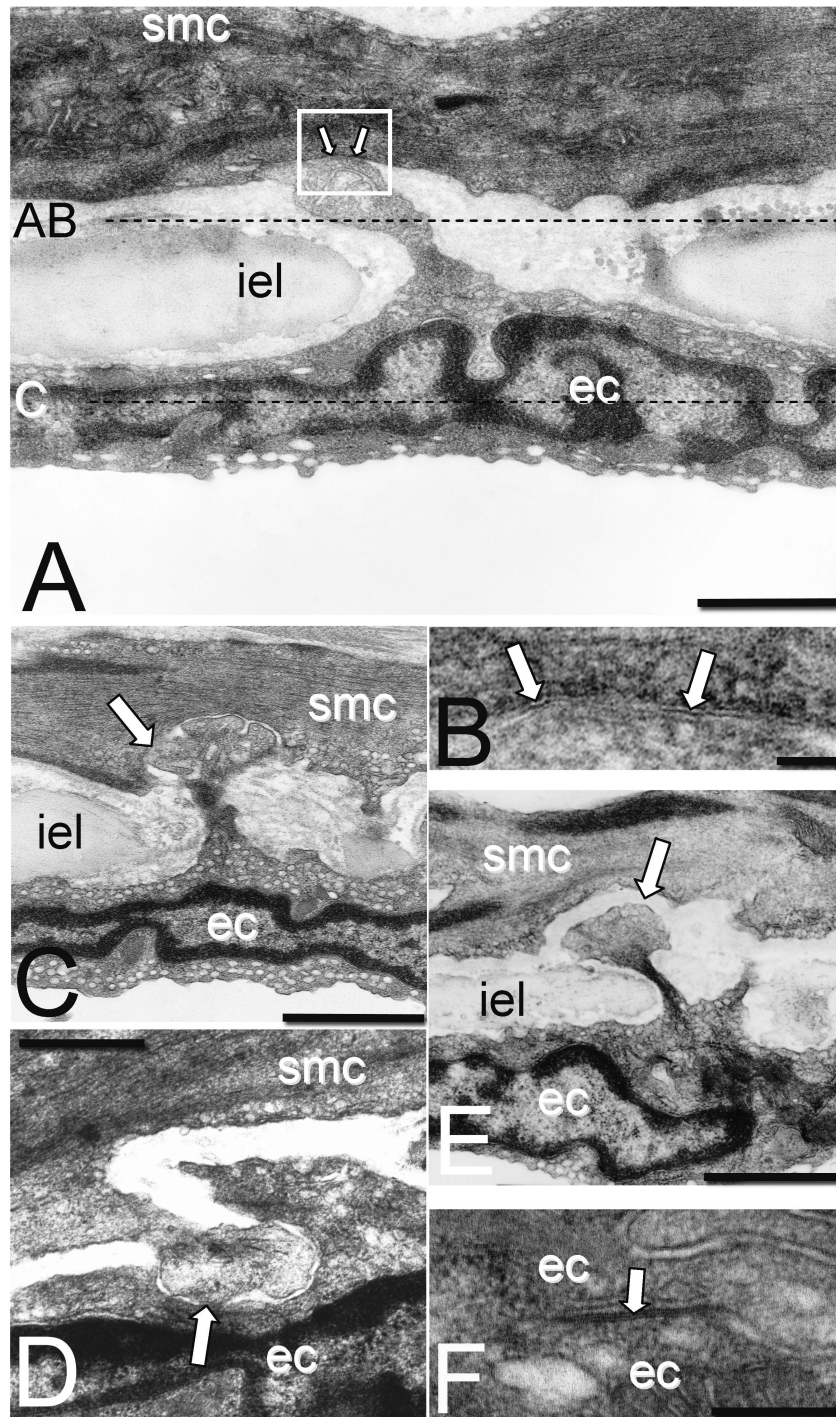


Figure 8

